

NASA TECHNICAL NOTE



NASA TN D-2743

NASA TN D-2743

LOAN COPY: RLII
AFWL (WLIL-2)
KIRTLAND AFB, N



STUDIES OF FATIGUE CRACK GROWTH IN ALLOYS SUITABLE FOR ELEVATED-TEMPERATURE APPLICATIONS

by C. Michael Hudson
Langley Research Center
Langley Station, Hampton, Va.

NASA TN D-2743

TECH LIBRARY KAFB, NM



0079697

STUDIES OF FATIGUE CRACK GROWTH IN ALLOYS SUITABLE FOR
ELEVATED-TEMPERATURE APPLICATIONS

By C. Michael Hudson

Langley Research Center
Langley Station, Hampton, Va.

NATIONAL AERONAUTICS AND SPACE ADMINISTRATION

For sale by the Office of Technical Services, Department of Commerce,
Washington, D.C. 20230 -- Price \$1.00

STUDIES OF FATIGUE CRACK GROWTH IN ALLOYS SUITABLE FOR
ELEVATED-TEMPERATURE APPLICATIONS

By C. Michael Hudson
Langley Research Center

SUMMARY

Constant-amplitude axial-load fatigue-crack-propagation tests were conducted on 8-inch (20.3-cm) wide sheet specimens made of AM 350 (CRT) and AM 367 stainless steels, two thicknesses of Ti-8Al-1Mo-1V (duplex annealed) titanium alloy, 2020-T6, 2024-T81 (clad), and RR-58 (clad) aluminum alloys, and Inconel 718 superalloy. Tests were conducted at room, elevated, and cryogenic temperatures to determine the effect of temperature on crack propagation in each material.

The fatigue-crack-growth resistance of the materials was determined and compared with materials tested similarly in a previous investigation. At elevated temperature, the 0.050-inch (1.27-mm) thick titanium alloy, Ti-8Al-1Mo-1V, in either the duplex- or triplex-annealed condition showed the greatest resistance to crack growth. At the room and cryogenic temperatures, the superalloy Inconel 718 appeared to be the most resistant. The AM 367 stainless steel showed good resistance to crack growth at all temperatures but only a limited number of tests were conducted on this material.

INTRODUCTION

A study of the fatigue-crack-growth characteristics of nine materials having potential use in supersonic aircraft is reported in reference 1 which is extended herein to include seven additional materials. Axial-load fatigue tests were conducted at positive mean stresses on 8-inch (20.3-cm) wide sheet specimens. Identical tests were conducted at elevated, room, and cryogenic temperatures to determine the effect of temperature on fatigue crack growth.

The experimental results of this study are presented in this paper. The effects of temperature on crack propagation in each material were determined. In addition, the crack-growth characteristics of the seven materials tested are compared with the characteristics of the most resistant materials tested in the previous investigation (ref. 1) to provide a comprehensive ranking of each material with respect to resistance to fatigue crack propagation.

SYMBOLS

The units used for the physical quantities defined in this paper are given both in the U.S. Customary Units and in the International System of Units (SI). Factors relating the two systems are given in reference 2.

a	one-half of the total length of a central symmetrical crack, inches or centimeters (cm)
N	number of cycles
S _a	alternating stress amplitude, ksi or meganewton/meter ² (MN/m ²)
S _m	mean stress, ksi or meganewtons/meter ² (MN/m ²)
t	specimen thickness, inch or millimeters (mm)

TESTS

Specimens

The materials tested in this investigation are listed in the following table:

Material	Condition	Thickness	
		in.	mm
Stainless steel	AM 350 (CRT)	0.050	1.27
Stainless steel	AM 367	.050	1.27
Aluminum alloy	2020-T6	.050	1.27
Aluminum alloy	2024-T81 (clad)	.063	1.61
Aluminum alloy	RR-58 (clad)	.063	1.61
Titanium alloy	Ti-8Al-1Mo-1V (duplex annealed)	.050	1.27
Titanium alloy	Ti-8Al-1Mo-1V (duplex annealed)	.250	6.35
Superalloy	Inconel 718	.050	1.27

All the specimens for each alloy were obtained from the same mill heat. The tensile properties of each material tested are listed in table I and the nominal chemical compositions, in table II.

The general configuration of the specimens may be seen in figure 1. The specimens were 24 inches (61 cm) long and 8 inches (20.3 cm) wide. All specimens were made with the longitudinal axis of the specimens parallel to the

grain of the sheet. A 0.1-inch (0.254-cm) notch was cut into the center of each specimen by means of an electrical discharge process. Very localized heating occurs in making notches in this manner. Thus, virtually all of the material through which the fatigue crack propagates is unaltered by the cutting process.

Prior to shearing the specimen blanks, the sheet materials were covered with tape to protect the surfaces. Following shearing, all specimens were chemically cleaned. Those specimens requiring heat treatment were then heat treated according to the procedures outlined in table III.

A reference grid (fig. 2) was photographically printed on the specimen surfaces to define intervals along the crack path. This photographic method produces no mechanical defects in the specimen surface, and, consequently, no stress concentrations are introduced. Metallographic examination and tensile tests conducted on specimens bearing the grid indicate that the grid had no detrimental effects upon the materials tested.

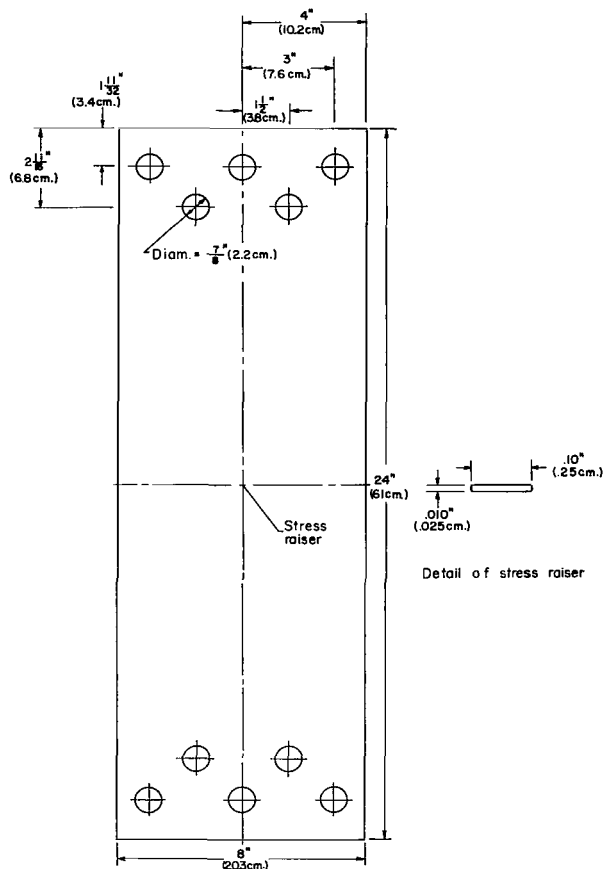


Figure 1.- Specimen configuration for crack propagation studies.

Testing Equipment

Three axial-load fatigue testing machines were employed in this investigation. A 20 000-pound (89-kN) capacity subresonant fatigue machine (ref. 3) having an operating frequency of 1800 cpm (30 Hz) was used for tests expected to last more than 1 000 000 cycles. A 100 000-pound (445-kN) capacity hydraulic fatigue machine which applied loads at a rate of 1200 cpm (20 Hz) was employed in tests expected to last from 10 000 to 1 000 000 cycles. A combination hydraulic and subresonant fatigue testing machine (ref. 4) capable of applying loads up to 132 000 pounds (587 kN) hydraulically or 110 000 pounds (489 kN) subresonantly was used as the needs for testing dictated. The operating frequencies were 40 to 60 cpm (0.7 to 1 Hz) for the hydraulic unit, and approximately 820 cpm (14 Hz) for the subresonant unit.

In all tests, loads were monitored by measuring the output of a bridge circuit whose active elements were wire-resistance strain gages. These gages were fixed to weigh bars through which the load was transmitted to a specimen. Monitoring precision was approximately ± 1 percent.

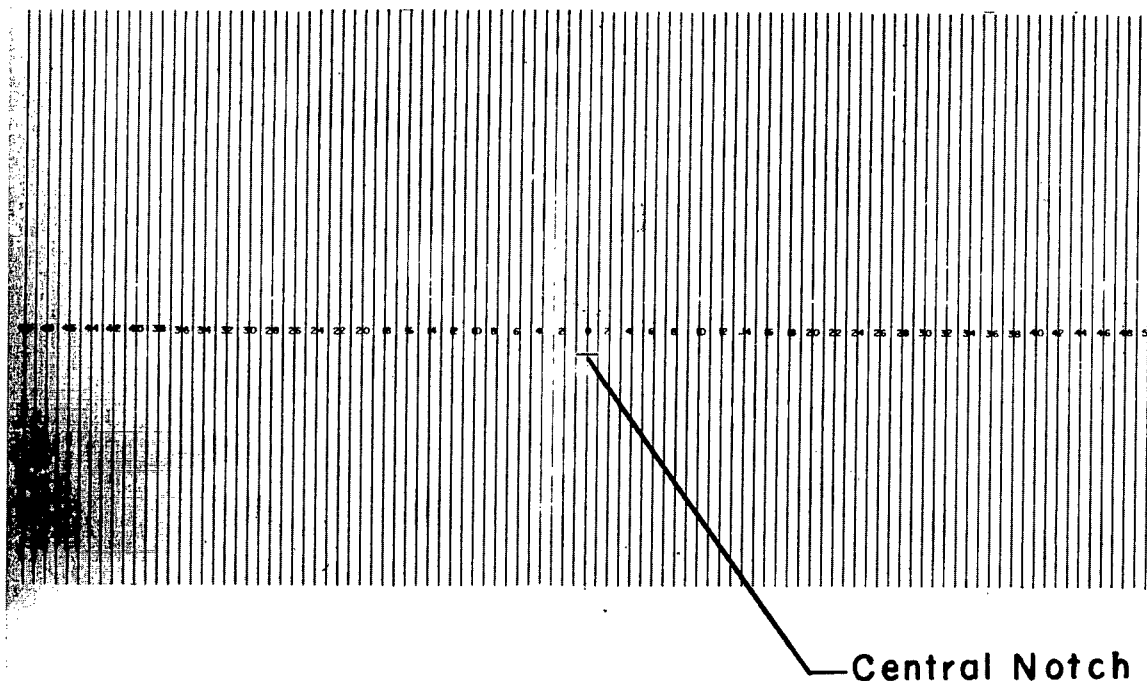
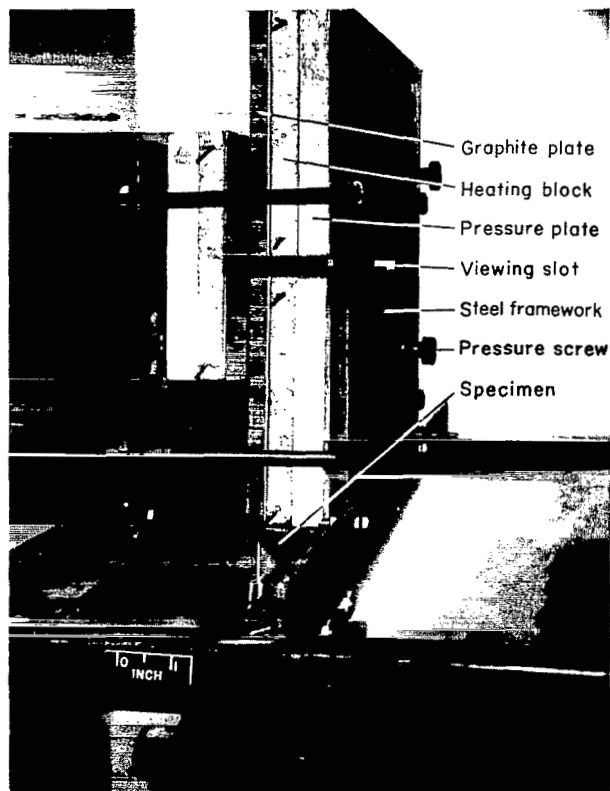


Figure 2.- Grid used to mark intervals in crack path. Grid spacing is 0.05 inch (1.27 mm). L-63-4299.1

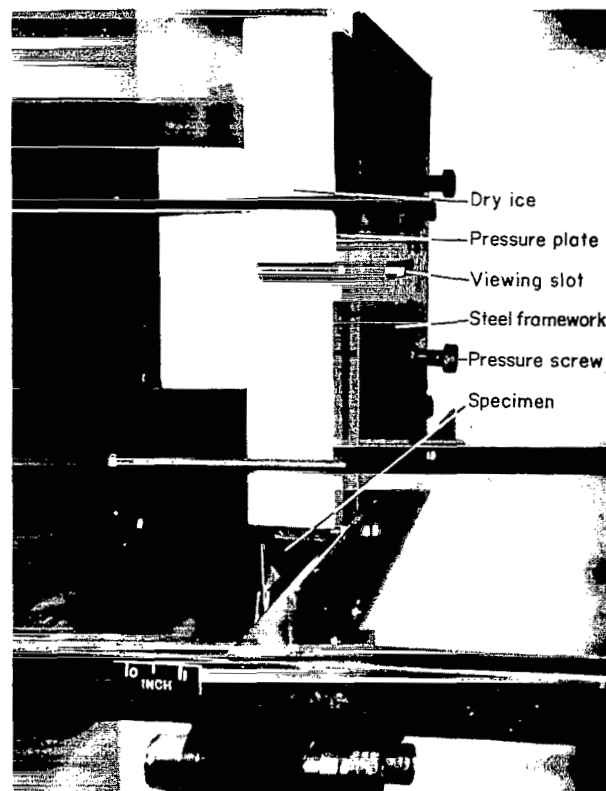
The apparatus used in the elevated-temperature tests (fig. 3) consisted of three heating units and a steel framework which held the heating units in contact with the specimen. The heating units were composed of a 1/2-inch (1.27-cm) thick graphite plate, a ceramic block containing wire resistance heaters, and an insulating pressure plate. A machine screw was jammed against the insulating pressure plate to hold the heating unit in contact with the specimen surface. The screws were carefully tightened to insure thermal contact without introducing significant frictional forces. Two heating units were placed on the observation side of the specimen; one above and the other below the region of crack growth. A 1/2-inch (1.27-cm) gap was provided to insure an unobstructed view of the propagating crack. The third unit was located on the opposite surface immediately opposite the crack-growth region.

A control thermocouple was fixed in the expected crack path near the edge of the specimen. By using an edge control point, the temperature was found to vary $\pm 5^{\circ}$ F ($\pm 3^{\circ}$ K) across the specimen width. The temperature at a given point was found to vary $\pm 2^{\circ}$ F ($\pm 1^{\circ}$ K) during the course of the test. Temperature control was maintained in the elevated-temperature tests by a controller-recorder which regulated current flow through a saturable reactor. The controller operated at 208 volts using 60-cycle single-phase ac power.

The equipment used in the -109° F (195° K) tests (fig. 4) consisted of three blocks of dry ice, the same steel framework used for the furnace, and an insulating cover box. The dry ice blocks were mounted in the steel framework



L-63-9528.2
Figure 3.- Elevated-temperature-test apparatus.



L-63-9529.2
Figure 4.- Cryogenic-temperature-test apparatus.

and held in contact with the specimen surface in the same manner as the heating units. Test temperature was governed by the sublimation temperature of the dry ice and was found to vary less than 5° F (3° K).

The entire cooling apparatus was isolated from circulating air drafts by the insulating cover box. This isolation was necessary in order to control the sublimation rate of the dry ice satisfactorily. The specimen surfaces were periodically sprayed with ethyl alcohol to prevent frost buildup in the crack-growth region.

Specimens were clamped between $3/8$ -inch (0.95-cm) thick aluminum guides (ref. 5) to prevent buckling and out-of-plane vibrations in all the room-temperature tests. Guides were also used in the elevated- and cryogenic-temperature tests in which compressive loadings were applied. In these latter tests, the heating or cooling units were placed directly against the guide plates and the specimen was heated or cooled by heat conduction through the guides. Good temperature control was maintained throughout these tests.

Specimen surfaces were lubricated with light oil in the room- and cryogenic-temperature tests and with dry molybdenum disulfide in the elevated-temperature tests. One side of the guide contained a 1/2-inch (1.27-cm) cutout across its width to allow visual observation of the crack path. A transparent plate was fitted into the guide cutout to prevent buckling of the specimen.

Test Procedure

Constant-amplitude axial-load fatigue tests were conducted at positive mean stresses of 40 ksi (276 MN/m²) for AM 350, AM 367, and Inconel 718; 25 ksi (173 MN/m²) for Ti-8Al-1Mo-1V; and 15 ksi (104 MN/m²) for 2020-T6, RR-58 (clad), and 2024-T81 (clad). All stresses mentioned herein refer to the original net area of the specimen. Alternating stresses ranged from ± 60 to ± 5 ksi (± 414 to ± 30 MN/m²) for AM 350, AM 367, and Inconel 718; ± 25 to ± 2 ksi (± 173 to ± 14 MN/m²) for Ti-8Al-1Mo-1V; and ± 15 to ± 2 ksi (± 104 to ± 14 MN/m²) for 2020-T6, RR-58 (clad), and 2024-T81 (clad). Mean and alternating loads were kept constant throughout each test.

Tests were conducted at 80° F (300° K) and -109° F (195° K) on all materials, at 550° F (561° K) on the stainless steels, titanium alloys, and the superalloy, and at 250° F (394° K) on the aluminum alloys. Specimens were tested at the same stress levels at all test temperatures in order to evaluate the effect of temperature on crack propagation.

The test data were obtained by observing the crack growth through 30 power microscopes while illuminating the specimen with stroboscopic light. The number of cycles required to propagate the crack to each grid line was recorded so that the rate of crack propagation could be determined. Tests were terminated when the cracks reached a predetermined crack length, and the specimens were reserved for the subsequent residual static-strength investigation reported in reference 6.

RESULTS AND DISCUSSION

The crack-propagation-test results are presented in table IV which gives the number of cycles required to propagate a crack from a half length a of 0.15 inch (0.38 cm). The number of cycles given in table IV, and in figures 5 to 12, is the mean number of cycles required to grow cracks of equal length on both sides of the central starter notch. The numbers of cycles are referenced from a half crack length of 0.15 inch (0.38 cm) because at this length the fatigue crack growth is no longer influenced by the starter notch (ref. 7).

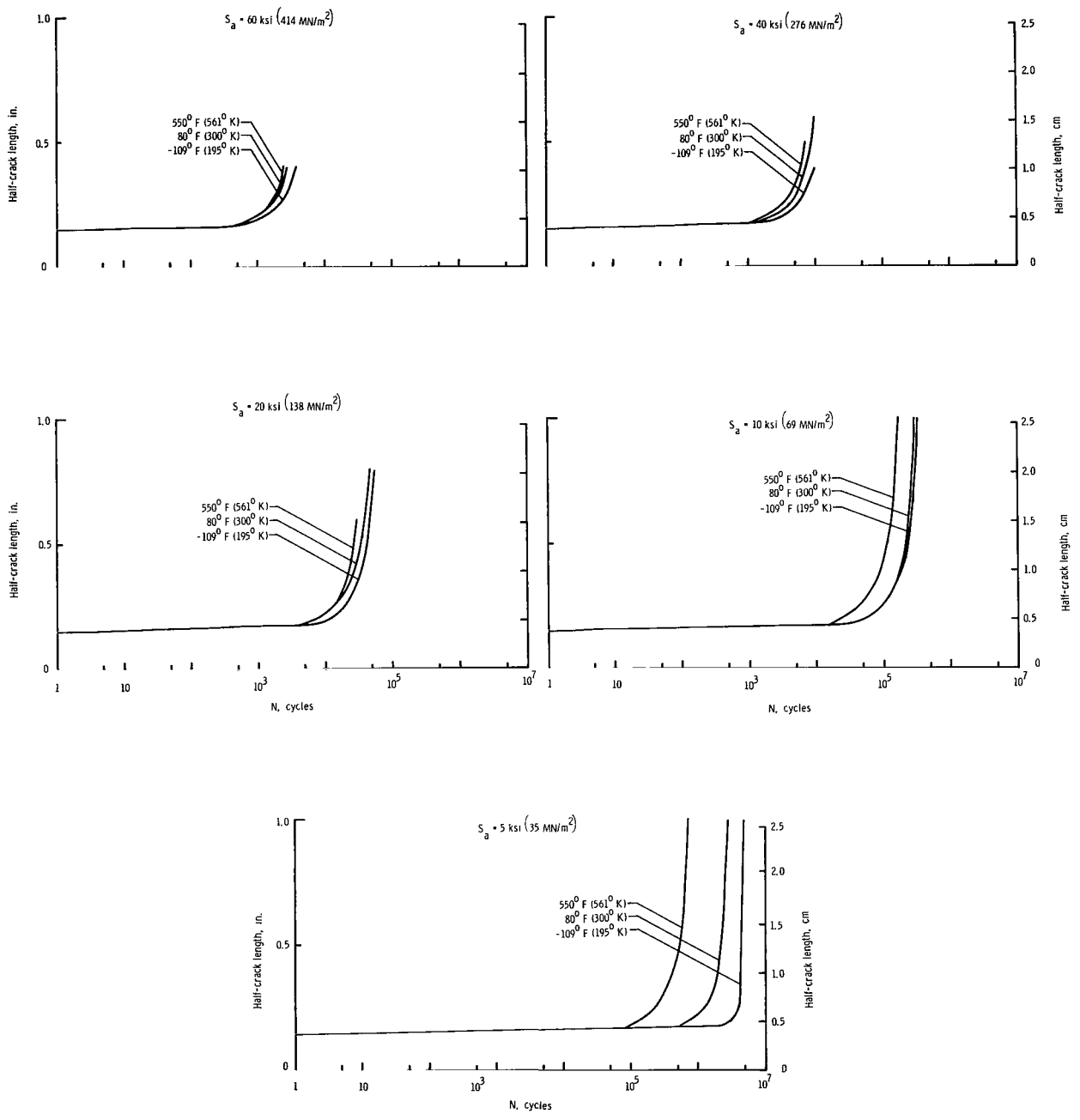


Figure 5.- Fatigue-crack-propagation curves for Inconel 718. $S_m = 40 \text{ ksi } (276 \text{ MN/m}^2)$.

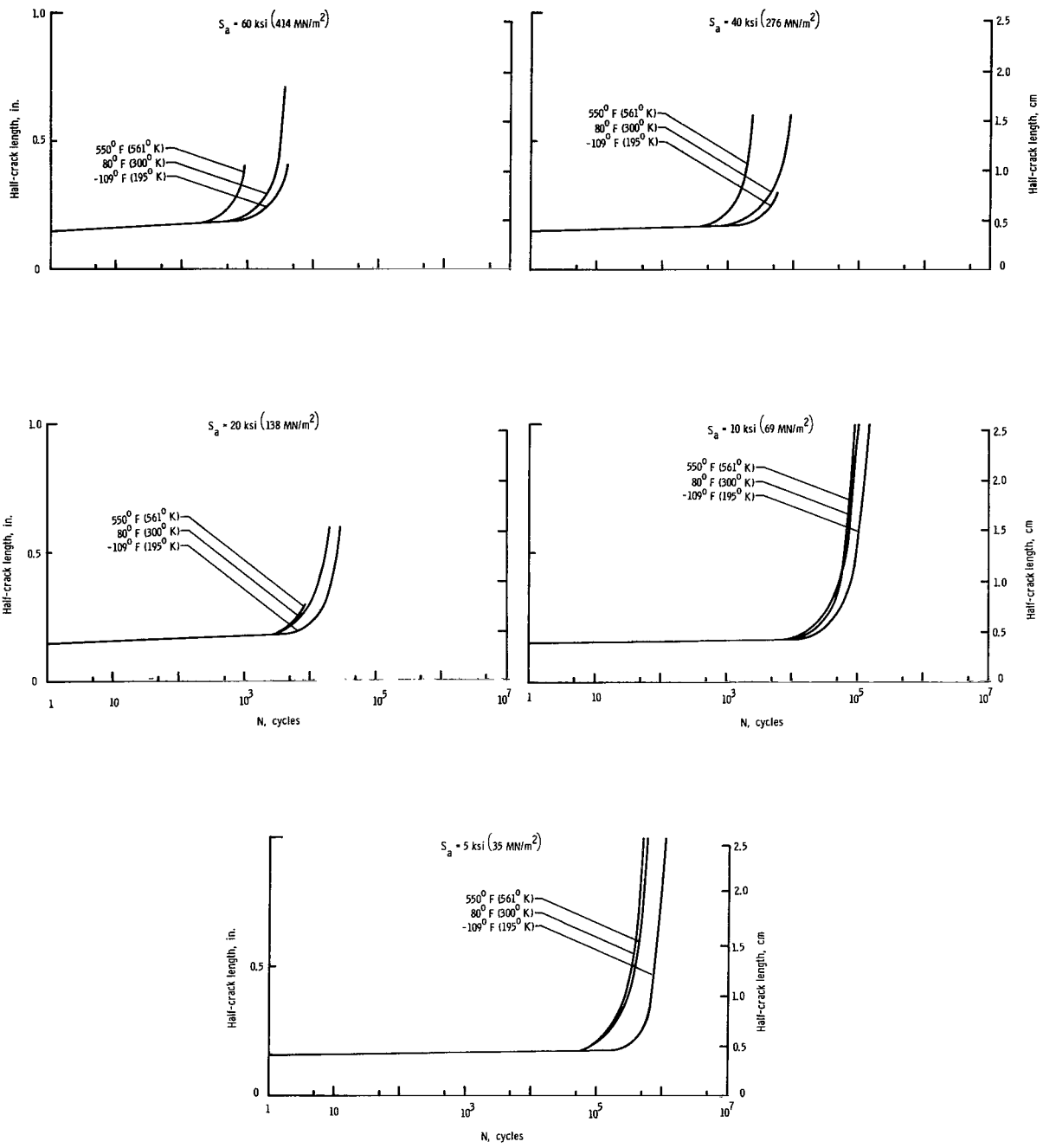


Figure 6.- Fatigue-crack-propagation curves for AM 350 (CRT). $S_m = 40 \text{ ksi (276 MN/m}^2\text{)}$.

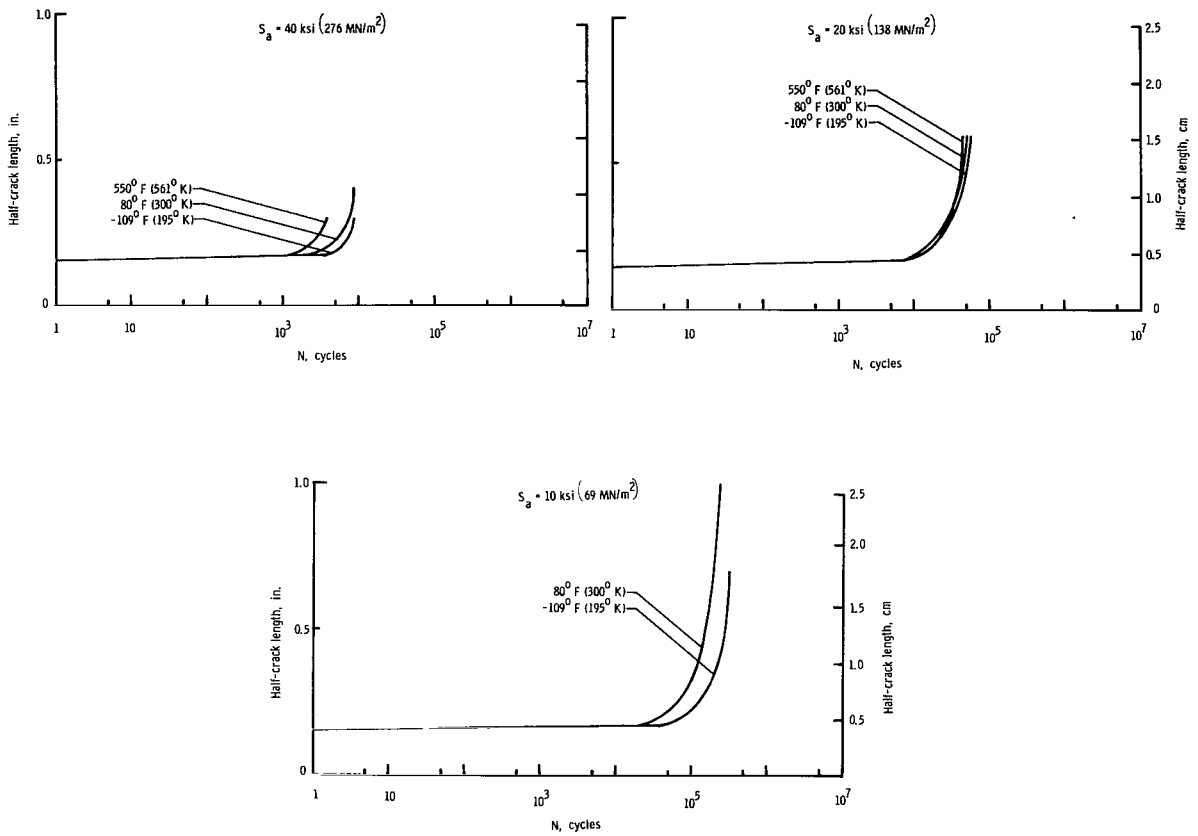


Figure 7.- Fatigue-crack-propagation curves for AM 367. $S_m = 40 \text{ ksi} (276 \text{ MN/m}^2)$.

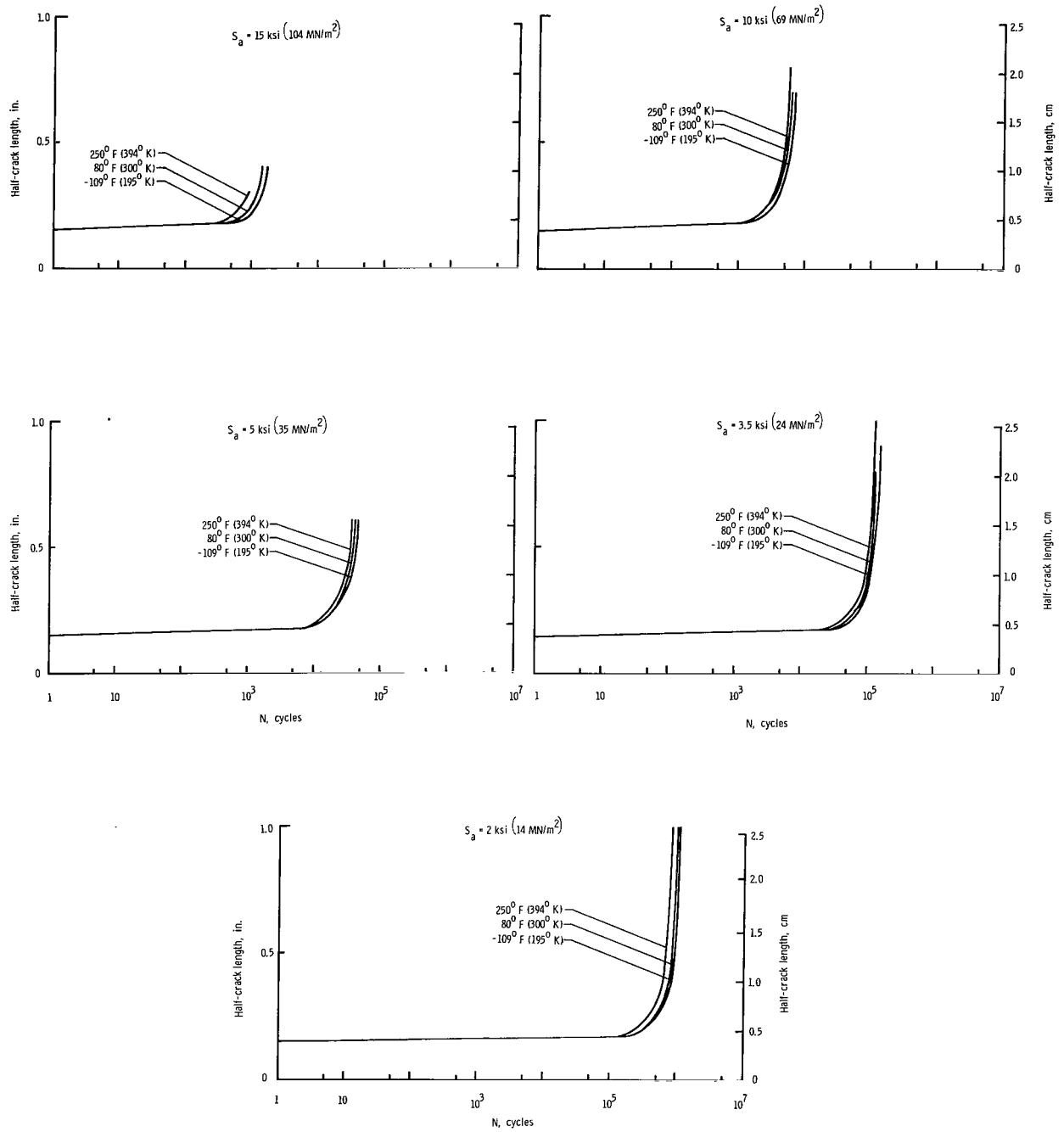


Figure 8.- Fatigue-crack-propagation curves for 2024-T81 (clad). S_m = 15 ksi (104 MN/m²).

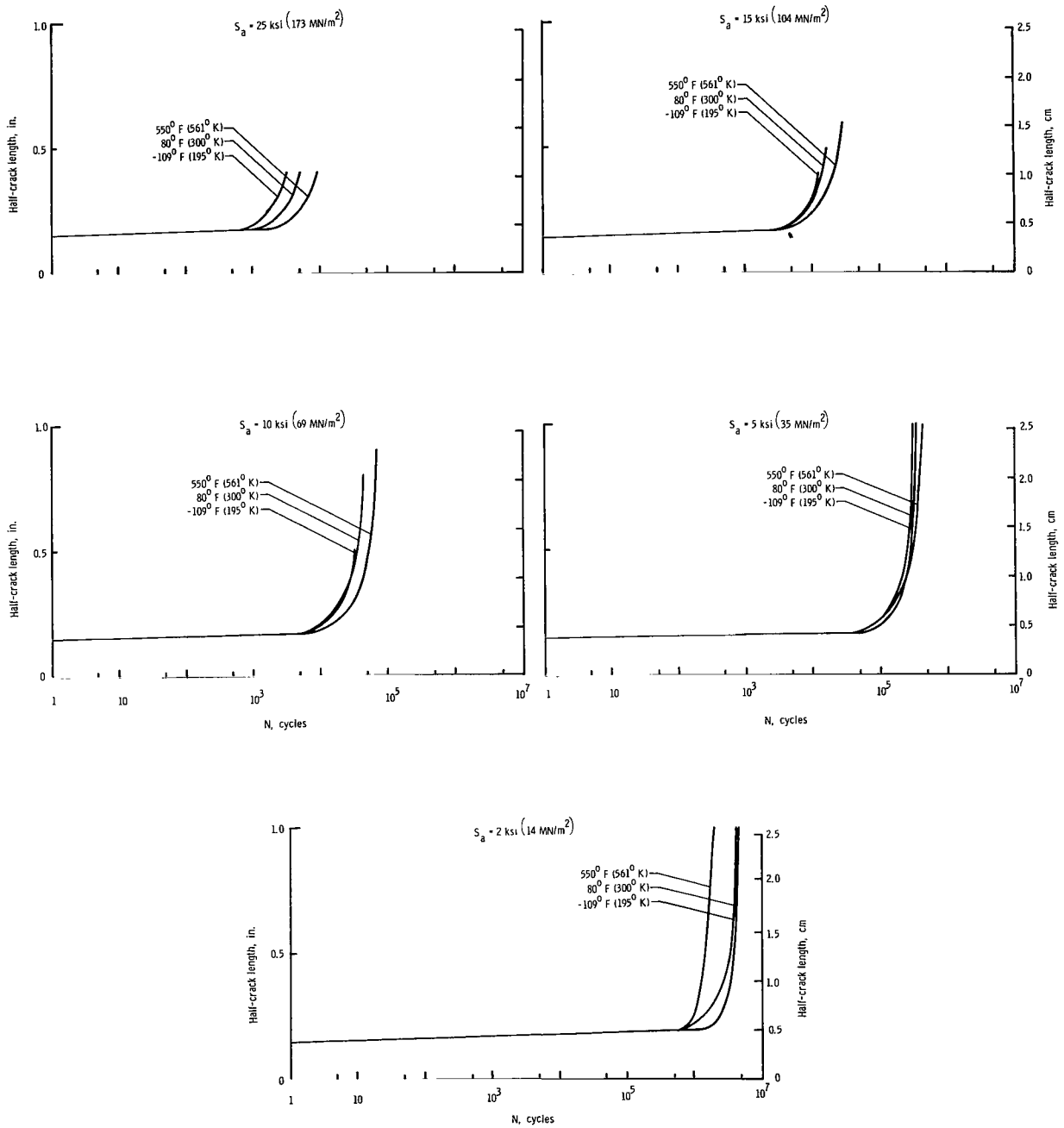


Figure 9.- Fatigue-crack-propagation curves for Ti-8Al-1Mo-1V (duplex annealed).
 $t = 0.050 \text{ inch (1.270 mm)}$; $S_m = 25 \text{ ksi (173 MN/m}^2\text{)}$.

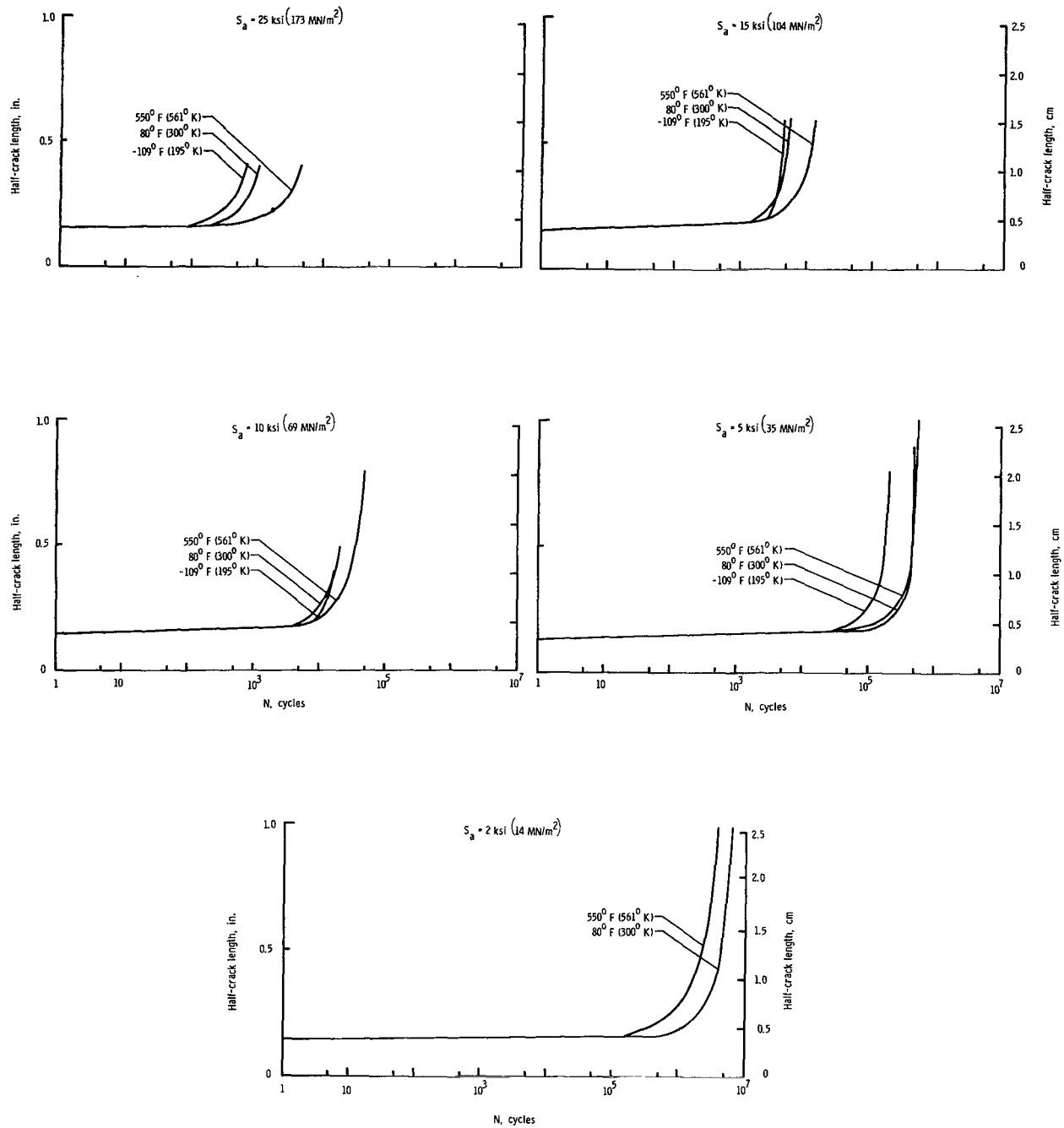


Figure 10.- Fatigue-crack-propagation curves for Ti-8Al-1Mo-1V (duplex annealed).
 $t = 0.250 \text{ inch (6.350 mm)}$; $S_m = 25 \text{ ksi (173 MN/m}^2\text{)}$.

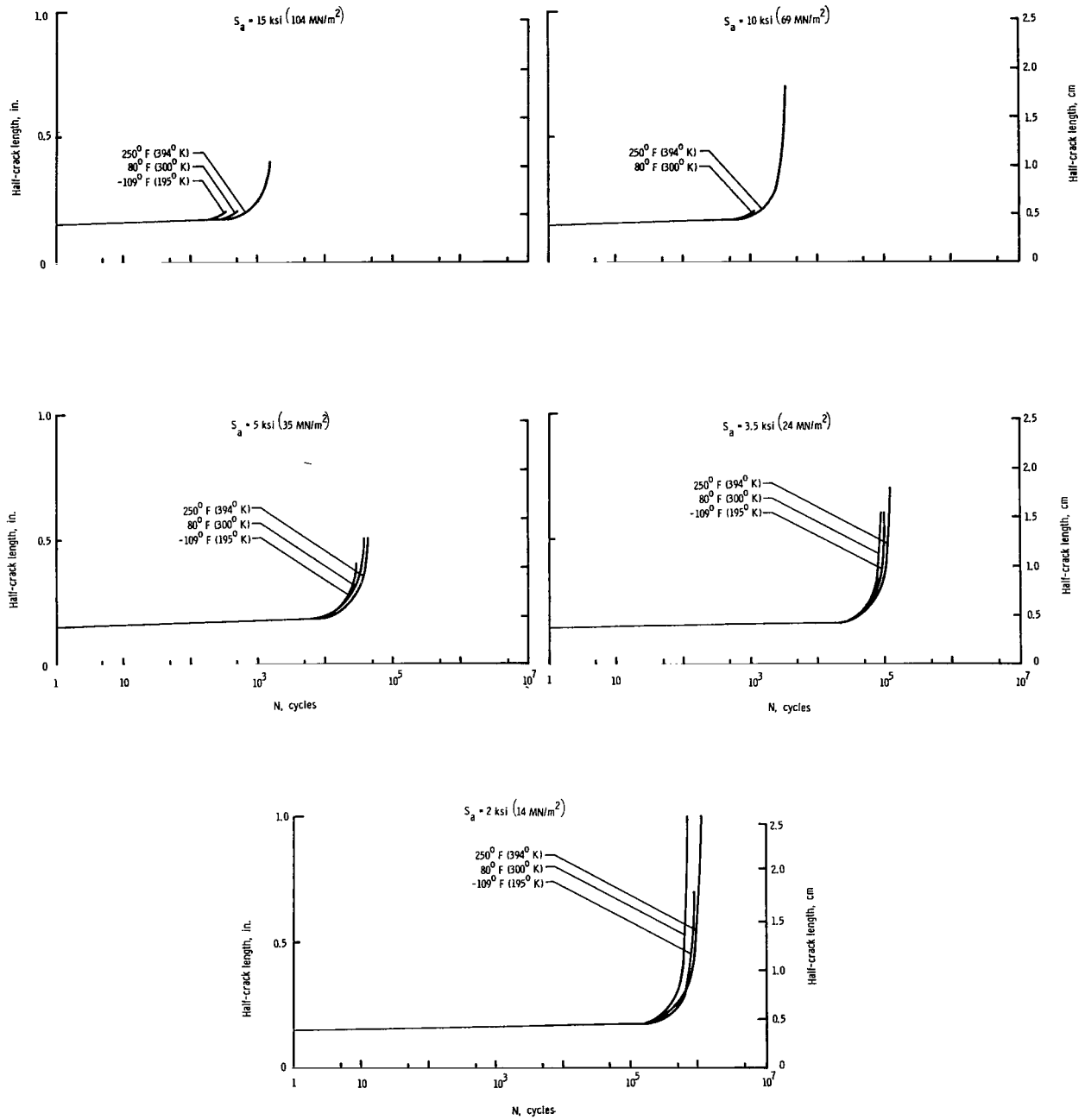


Figure 11.- Fatigue-crack-propagation curves for 2020-T6. $S_m = 15 \text{ ksi } (104 \text{ MN/m}^2)$.

Temperature Effect

The effect of temperature on crack growth was determined by comparison of the crack propagation curves from tests at room, elevated, and cryogenic temperatures. The crack-growth curves for Inconel 718, AM 350, AM 367, and 2024-T81 (clad) (figs. 5, 6, 7, and 8, respectively) show almost without exception that the higher the temperature, the more rapidly fatigue cracks propagated. A similar change of crack-growth resistance with temperature was found for the stainless steels and a superalloy tested in the previous crack-growth investigation (ref. 1). The loss of resistance to fatigue crack growth with increasing temperature may be attributed to the normal deterioration of properties at elevated temperature.

The crack-growth curves for both thicknesses of Ti-8Al-1Mo-1V (duplex annealed) and for 2020-T6 (figs. 9, 10, and 11, respectively) indicate that fatigue cracks generally grow most slowly at elevated temperature, and most rapidly at cryogenic temperature. In most instances, however, the differences between the crack-growth curves were small. The titanium alloys tested in reference 1 were also found to be slightly more resistant to crack growth at elevated temperature.

The fatigue-crack-growth curves for the RR-58 (clad) (fig. 12) indicate no consistent variation of crack-growth resistance with temperature. At the higher stress levels the RR-58 (clad) showed the greatest resistance at room temperature, while at the lower stress levels the resistance was greatest at 250° F (394° K).

Crack-Growth Resistance of Materials

The relative crack-growth resistance of the various materials was determined by comparing plots of the rates of fatigue crack growth against the ratio of the alternating to the mean stress (i.e., the stress ratio). The lower the rate of crack growth for a given stress ratio, the greater the resistance of the material to fatigue crack growth. The crack-growth rates were determined graphically by taking the slopes of the fatigue-crack-growth curves (on a linear plot) at different crack lengths. Figures 13, 14, and 15 show the rate plotted against stress ratio for the elevated-, room-, and cryogenic-temperature tests, respectively. The rates shown in these three figures are for a half crack length a of 0.40 inch (1.02 cm). The materials generally maintained the same relative positions at other crack lengths.

The mean stresses at which the comparisons in figures 13 to 15 were made are approximately one-fifth of the ultimate tensile strength of the materials. The mean stress-density ratios for the materials are also approximately equal.

At elevated temperature (fig. 13), the thin titanium sheet showed the greatest resistance to crack growth, followed by Inconel 718, and the thick titanium plate. The results of tests on AM 367 indicate good crack-growth resistance at elevated temperature, but only a small number of tests were conducted. Fatigue-crack-growth rates in the 2020-T6, RR-58 (clad), 2024-T81 (clad), and AM 350 were relatively high.

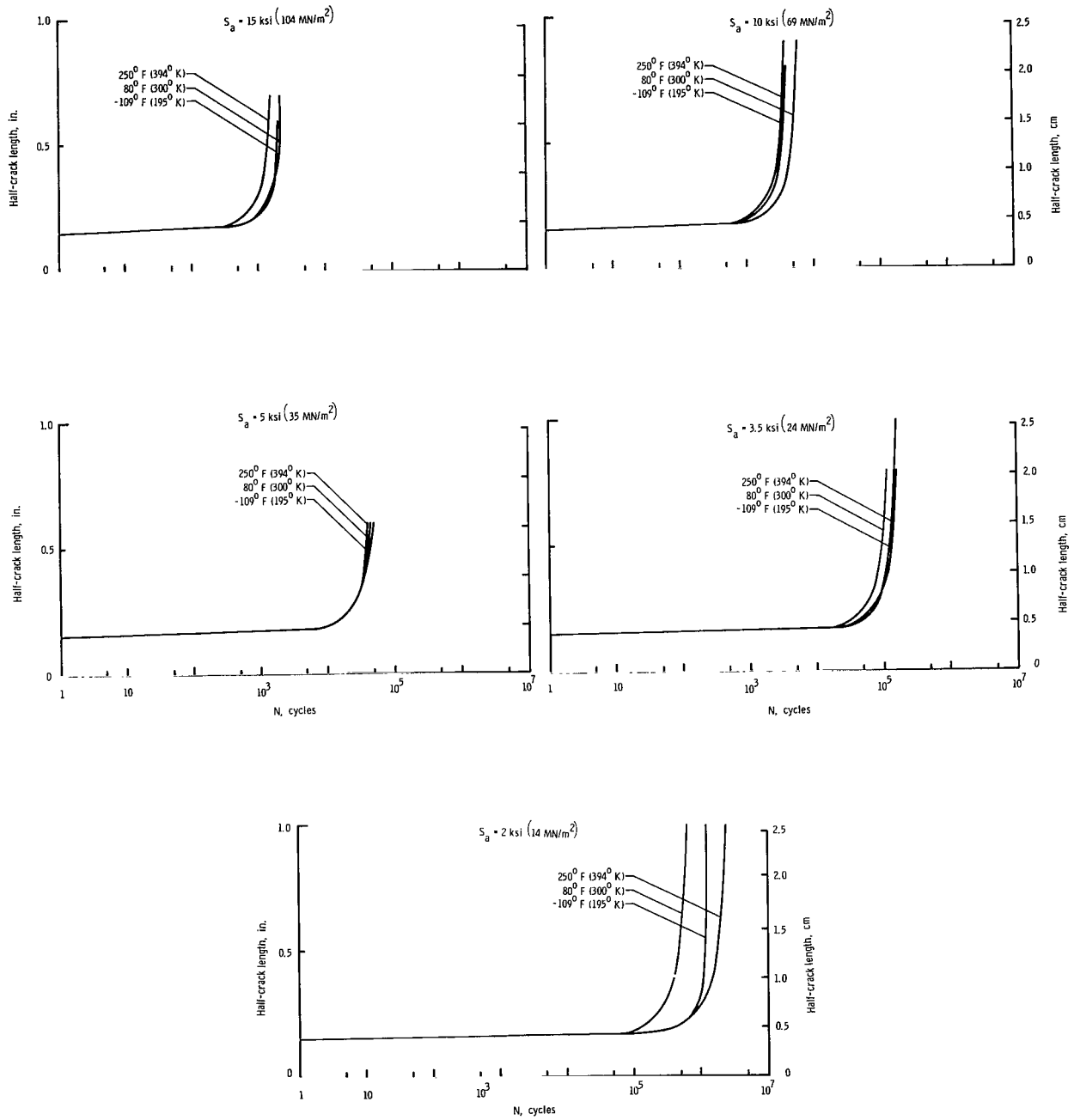


Figure 12.- Fatigue-crack-propagation curves for RR-58 (clad). S_m = 15 ksi (104 MN/m²).

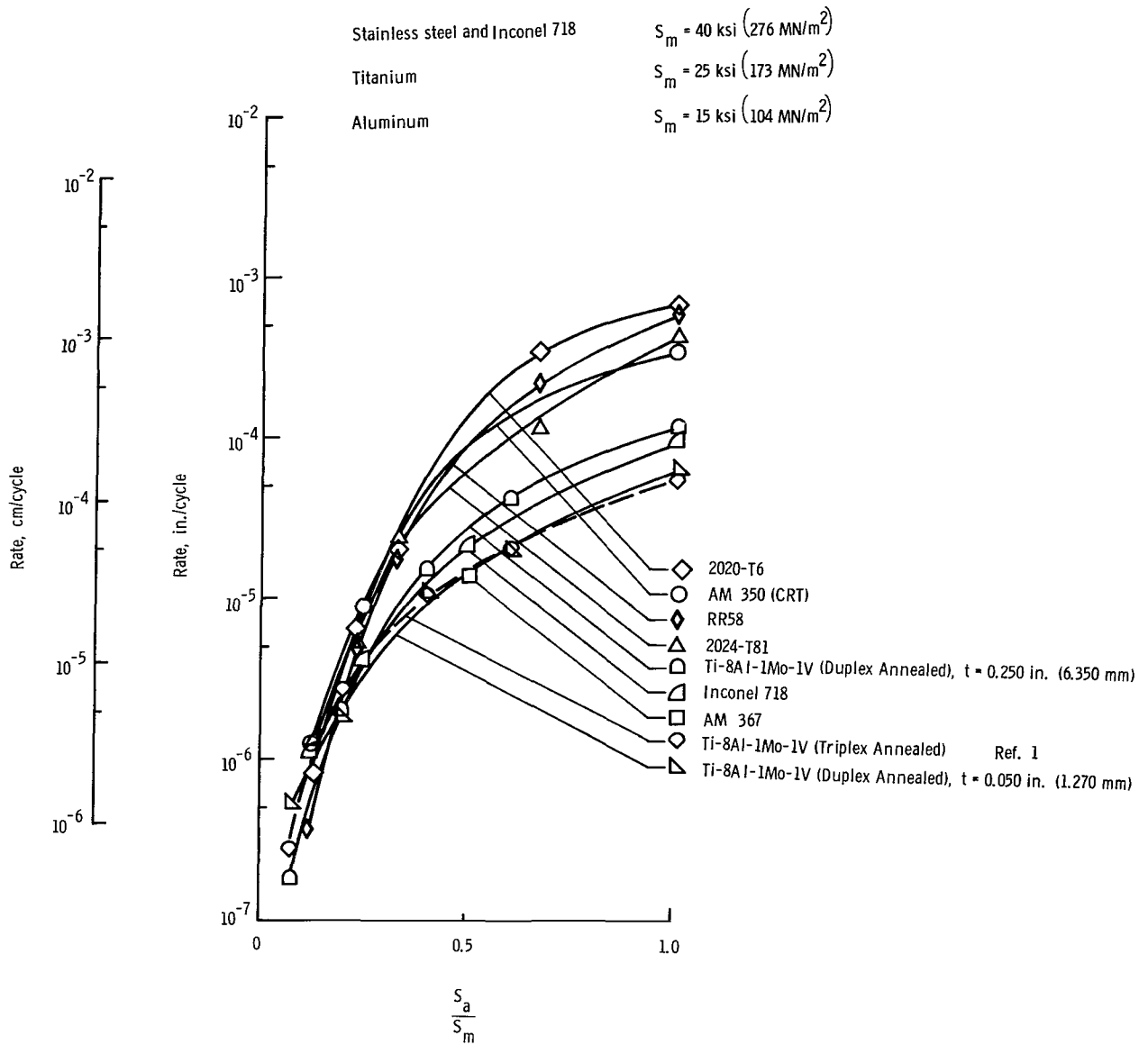


Figure 13.- Fatigue-crack-propagation rate as a function of the ratio of alternating to mean stress at elevated temperature (250° F (394° K) for the aluminums, 550° F (561° K) for all others) for a half crack length a of 0.40 inch (1.02 cm).

Data from tests at 550° F (561° K) and at 250° F (394° K) are compared directly in figure 13 in order to evaluate the relative efficiencies of the various materials at the approximate elevated temperature extremes to which the materials might be subjected in supersonic aircraft.

At room temperature (fig. 14), Inconel 718 and AM 367 exhibited the lowest fatigue-crack-growth rates followed by AM 350 and the thin titanium sheet. The crack-growth rates again were quite high for the three aluminum alloys and also

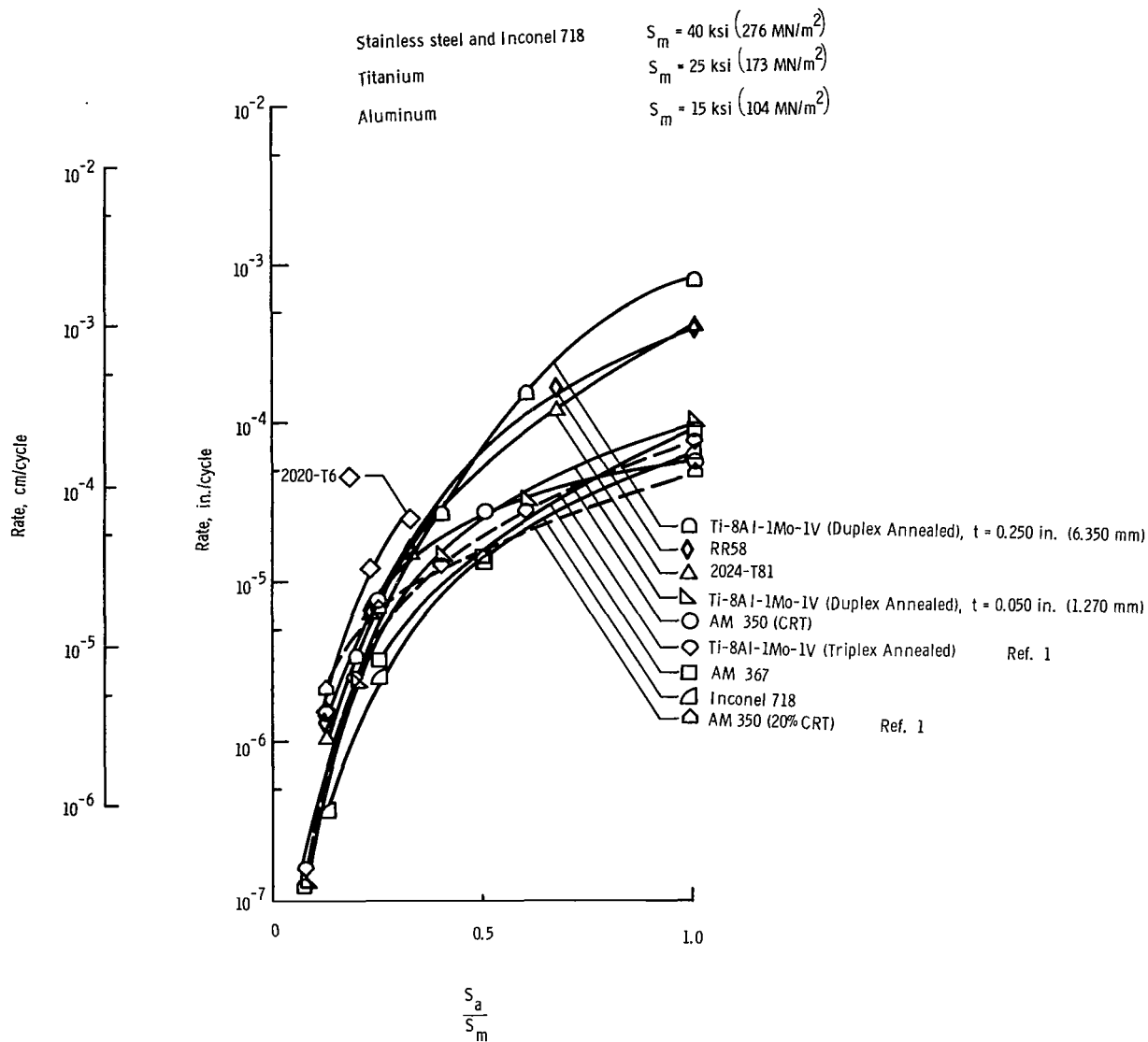


Figure 14.- Fatigue-crack-propagation rate as a function of the ratio of alternating to mean stress at 80° F (300° K) for a half crack length a of 0.40 inch (1.02 cm).

for the thick titanium plate. The AM 367 and Inconel 718 (fig. 15) also showed the greatest resistance to fatigue crack growth at cryogenic temperature. The AM 350 and the thin titanium sheet followed. The three aluminum alloys and the thick titanium plate were once again the least resistant materials tested.

Thus, it appears that over the temperature range of the investigation, the Inconel 718 and the AM 367 exhibited the greatest overall resistance to fatigue crack growth. It should be remembered, however, that a somewhat smaller quantity of data was obtained on the AM 367. It further appears that the crack-growth resistance of the thick titanium plate is considerably lower than the resistance of the thin sheet. This lower crack-growth resistance may result

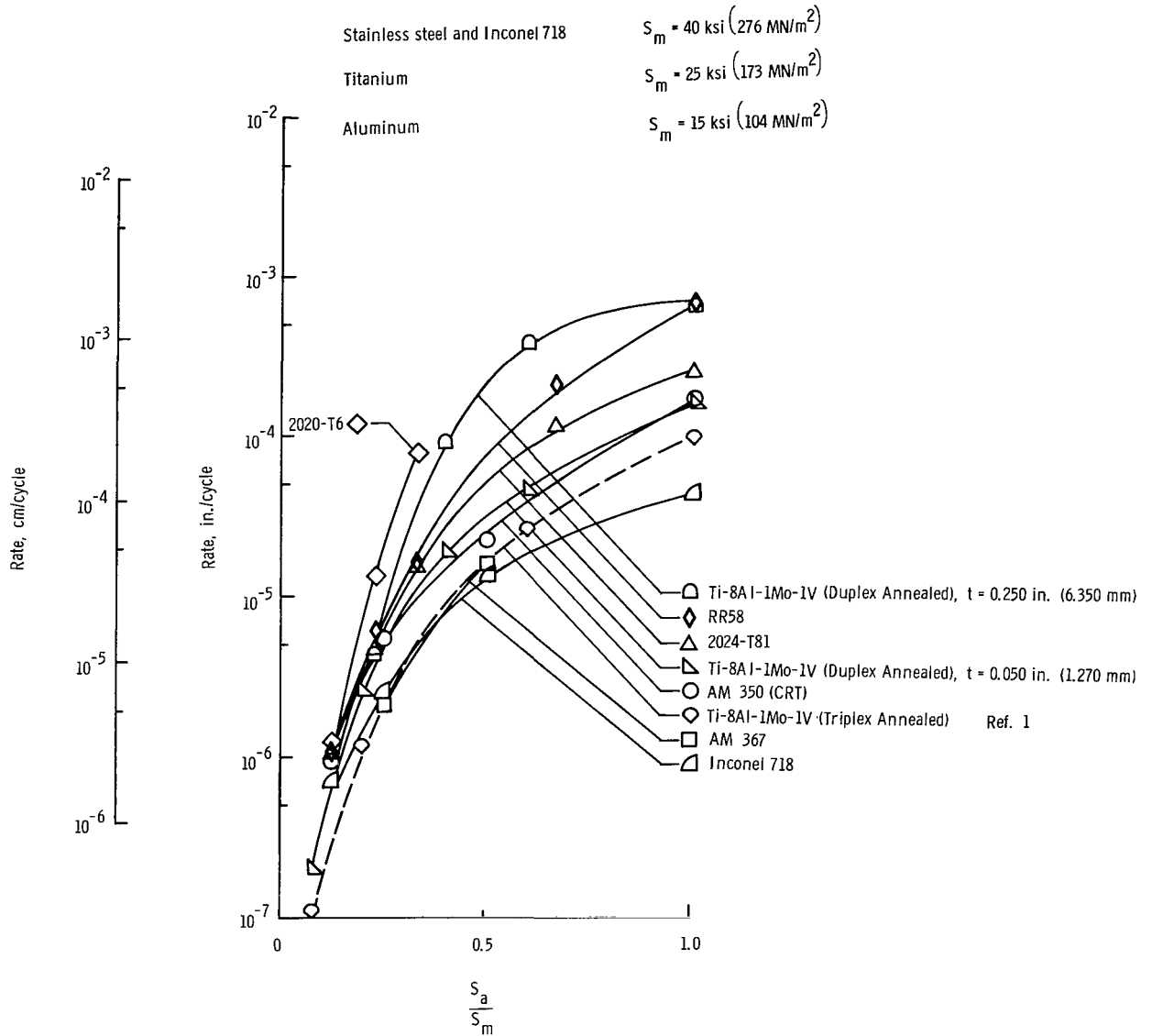


Figure 15.- Fatigue-crack-propagation rate as a function of the ratio of alternating to mean stress at $-109^\circ \text{ F } (195^\circ \text{ K})$ for a half crack length a of 0.40 inch (1.02 cm).

from a tri-axial stress state inherent in the thicker material. In this state, the plastic deformation in the material ahead of the crack tip is partially restrained by the large bulk of elastic material surrounding the plastic zone. This restraint of plastic flow causes the stresses in this plastic zone to increase to a higher level than would be possible if plastic flow could occur readily, as in thin sheet materials. These higher stresses could promote a faster rate of fatigue crack growth. The difference between crack-growth resistance of the thick and the thin titanium material could also have resulted from the different amounts of working to which the material was subjected in processing.

For purposes of comparison, the crack-growth-rate against stress-ratio curves for sheet Ti-8Al-1Mo-1V (triplex annealed) titanium alloy, and AM 350 (20% CRT) stainless steel, which showed the greatest crack-growth resistance in the previous investigation (ref. 1), have been included (dashed curves) with the test data reported herein. Inspection of figures 13, 14, and 15 indicates that for the entire spectrum of materials tested, the sheet Ti-8Al-1Mo-1V titanium alloy in either the duplex- or triplex-annealed condition has the greatest resistance to fatigue crack growth at elevated temperature. At the room and cryogenic temperatures, Inconel 718 generally appeared to be most resistant. The AM 367 also exhibited relatively good crack-growth characteristics at all three test temperatures.

The data for the triplex-annealed titanium alloy has been included at all three test temperatures to show the effect of the different annealing processes on the crack-growth resistance. The curves indicate that at elevated temperature the crack-growth characteristics of the triplex-annealed alloy are approximately equal to those of the duplex-annealed alloy. At the room and cryogenic temperatures, the triplex-annealed alloy is generally more resistant to crack growth than is the duplex-annealed alloy.

CONCLUSIONS

The following conclusions were drawn from the investigation of the fatigue-crack-growth characteristics of seven materials considered for structural applications in supersonic aircraft design. Tests were conducted at temperatures of -109° F (195° K), 80° F (300° K), and either 550° F (561° K) or 250° F (394° K) depending upon the material.

1. The higher the temperature the more rapidly fatigue cracks propagated in AM 350 (CRT) and AM 367 stainless steel, Inconel 718 superalloy, and 2024-T81 (clad) aluminum alloy. Cracks were found to grow more rapidly as the temperature decreased in the Ti-8Al-1Mo-1V (duplex annealed) titanium alloy and the 2020-T6 aluminum alloy. These conclusions concur in general with those presented in NASA Technical Note D-2331. The RR-58 (clad) aluminum alloy exhibited no consistent variation of crack-growth resistance with temperature.

2. The superalloy Inconel 718 exhibited the greatest overall resistance to fatigue crack growth. The 0.050-inch (1.27-mm) thick Ti-8Al-1Mo-1V (duplex annealed) sheet material was the most resistant to crack growth at elevated temperature followed by Inconel 718. The Inconel 718 showed the greatest resistance to crack propagation at room and cryogenic temperatures. A limited number of tests on AM 367 indicated this material has good resistance to crack growth, but only a small number of tests were conducted.

3. The fatigue-crack-growth resistance of the 0.250-inch (6.35-mm) thick Ti-8Al-1Mo-1V (duplex annealed) titanium alloy was considerably lower than the resistance of the 0.050-inch (1.27-mm) thick material. This lower resistance in the thicker material may result from a tri-axial stress state, or from a difference in the cold working.

4. For the test conditions used, the crack-growth resistance of the 2020-T6, RR-58 (clad), and 2024-T81 (clad) aluminum alloys was relatively poor over the entire temperature range.

5. Comparison of the crack-growth-rate with stress-ratio curves for the sheet Ti-8Al-1Mo-1V (duplex annealed) with similar curves for sheet Ti-8Al-1Mo-1V (triplex annealed) obtained in a previous investigation (TN D-2331), shows that crack-growth characteristics are quite similar at elevated temperature. However, at the room and cryogenic temperatures the triplex-annealed alloy was generally more crack-growth resistant than the duplex-annealed alloy.

Langley Research Center,
National Aeronautics and Space Administration,
Langley Station, Hampton, Va., January 6, 1965.

REFERENCES

1. Hudson, C. Michael: Fatigue-Crack Propagation in Several Titanium and Stainless-Steel Alloys and One Superalloy. NASA TN D-2331, 1964.
2. Mechtly, E. A.: The International System of Units - Physical Constants and Conversion Factors. NASA SP-7012, 1964.
3. Grover, H. J.; Hyler, W. S.; Kuhn, Paul; Landers, Charles B.; and Howell, F. M.: Axial-Load Fatigue Properties of 24S-T and 75S-T Aluminum Alloy as Determined in Several Laboratories. NACA Rept. 1190, 1954. (Supersedes NACA TN 2928.)
4. Hudson, C. Michael; and Hardrath, Herbert F.: Investigation of the Effects of Variable-Amplitude Loadings on Fatigue Crack Propagation Patterns. NASA TN D-1803, 1963.
5. Brueggeman, W. C.; and Mayer, M., Jr.: Guides for Preventing Buckling in Axial Fatigue Tests on Thin Sheet-Metal Specimens. NACA TN 931, 1944.
6. Figge, I. E.: Residual Strength of Alloys Potentially Useful in Supersonic Aircraft. NASA TN D-2613, 1965.
7. McEvily, Arthur J., Jr.; and Illg, Walter: The Rate of Fatigue-Crack Propagation in Two Aluminum Alloys. NACA TN 4394, 1958.
8. Weiss, V.; and Sessler, J. G., eds.: Aerospace Structural Metals Handbook. Volume II - Non-Ferrous Alloys. ASD-TDR-63-741, Vol. II, U.S. Air Force, Mar. 1963.

TABLE I.- AVERAGE TENSILE PROPERTIES OF MATERIALS TESTED

[Grain direction longitudinal]

Temperature		Ultimate tensile strength		Yield strength (0.2% offset)		Modulus of elasticity		Elongation, percent 2-in. (5.08-cm) gage length	Number of tests
°F	°K	ksi	MN/m ²	ksi	MN/m ²	ksi	GN/m ²		
AM 367									
-109	195	266.0	1835	263.7	1820	31.4 × 10 ³	217	5.0	3
80	300	243.4	1680	242.0	1670	30.7	212	4.2	3
550	561	206.1	1422	201.3	1389	20.1	139	3.8	3
AM 350 (CRT)									
-109	195	266.3	1838	222.0	1532	28.6 × 10 ³	197	20.7	3
80	300	223.4	1542	217.5	1501	27.8	192	16.2	3
550	561	197.8	1365	184.5	1273	22.5	155	3.0	3
Inconel 718									
-109	195	195.0	1346	161.2	1112	27.8 × 10 ³	192	28.0	3
80	300	193.7	1337	162.2	1119	27.8	192	23.3	3
550	561	172.1	1187	144.7	998	26.8	185	19.0	4
Ti-8Al-1Mo-1V (duplex annealed); t = 0.050 inch (1.27 mm)									
-109	195	178.0	1228	162.7	1123	17.7 × 10 ³	121	15.3	3
80	300	152.0	1049	133.6	922	18.3	126	12.5	3
550	561	115.5	797	93.7	647	14.1	97	12.0	3
Ti-8Al-1Mo-1V (duplex annealed); t = 0.250 inch (6.35 mm)									
-109	195	157.5	1087	145.6	1005	16.9 × 10 ³	117	11.0	3
80	300	137.4	948	120.0	828	14.8	102	17.3	3
550	561	113.8	785	85.8	592	13.3	92	16.5	2
2020-T6									
-109	195	88.3	609	82.4	569	12.4 × 10 ³	86	7.7	3
80	300	81.8	564	77.5	535	11.3	78	8.8	4
250	394	68.8	475	64.0	442	9.7	67	9.0	3
2024-T81 (clad)									
-109	195	69.0	476	62.2	429	8.8 × 10 ³	61	7.0	3
80	300	63.2	436	57.6	397	9.5	66	7.2	3
250	394	59.3	409	53.3	368	8.4	58	7.5	3
RR-58 (clad)									
-109	195	64.6	445	58.8	405	10.4 × 10 ³	72	8.3	3
80	300	59.2	408	54.6	377	10.0	69	7.0	3
250	394	54.0	372	51.3	354	10.5	72	7.3	3

TABLE II.- NOMINAL CHEMICAL COMPOSITION OF MATERIALS TESTED

Element	AM 367, percent	AM 350, percent	Inconel 718, percent	Ti-8Al-1Mo-1V, percent	2020-T6, percent	2024-T81 (clad), percent	RR-58 (clad), percent
C	0.021	0.08 to 0.12	0.10 max	0.08 max			
Mn	0.024	0.50 to 1.25	0.50 max		0.30 to 0.80	0.30 to 0.90	
P	0.002	0.040 max					
S	0.009	0.030 max					
Si	0.080	0.50 max	0.75 max		0.40 max	0.50 max	
Ni	3.40	4.00 to 5.00	50.0 to 55.0				1.2
Cr	14.25	16.00 to 17.00	17.0 to 21.0			0.10 max	
Mo	1.99	2.50 to 3.25	2.80 to 3.30	0.75 to 1.25			
V				0.75 to 1.25			
Al	0.03		0.20 to 1.00	7.50 to 8.50	Balance	Balance	Balance
N		0.07 to 0.13		0.05 max			
H				0.015 max			
Ti	0.35		0.30 to 1.30	Balance	0.10 max		0.1
Fe	Balance	Balance	Balance	0.30 max	0.40 max	0.50 max	1.0
Co	15.44						
Cu					4.0 to 5.0	3.8 to 4.9	2.5
Cb + Ta			4.50 to 5.75				
Li					0.9 to 1.7		
Mg					0.03 max	1.2 to 1.8	1.5
Zn					0.25 max	0.25 max	
Cd					0.10 to 0.35		

TABLE III.- MATERIAL HEAT TREATMENTS

Material	Condition	Heat treatment
AM 367	-----	Annealed 1400° F (1033° K), quench to -100° F (200° K) for 16 hr, aged 8 hr at 850° F (727° K), air cool
AM 350	CRT	20% cold rolled, tempered 3 to 5 min at 930° F (772° K), air cool
Inconel 718	-----	Annealed 1325° F (993° K) for 8 hr, furnace cool 20° F/hr to 1150° F (894° K), air cool
Ti-8Al-1Mo-1V	Duplex annealed	1450° F (1061° K) for 8 hr, furnace cool, 1450° F (1061° K) for 15 min, air cool
RR-58 (clad)	Fully heat treated to specification DTD 5070 A	5 min to 1 hr at 525° C to 530° C (798° K to 803° K), depending on gage, quench in cold water, 10 to 30 hr at 190° C ± 5° C (463° K ± 5° K)
2020	T6	See reference 8
2024 (clad)	T81	See reference 8

TABLE IV.- MEAN NUMBER OF CYCLES REQUIRED TO EXTEND CRACKS FROM A HALF-LENGTH OF 0.15 INCH (0.38 cm)

Temperature		S _a		Number of cycles required to propagate a crack from a half length a of 0.15 inch (0.38 cm) to a length a of -												
°F	°K	ksi	MN/m ²	0.20 in. (0.508 cm)	0.30 in. (0.762 cm)	0.40 in. (1.016 cm)	0.50 in. (1.270 cm)	0.60 in. (1.524 cm)	0.70 in. (1.778 cm)	0.80 in. (2.032 cm)	0.90 in. (2.286 cm)	1.00 in. (2.540 cm)	1.20 in. (3.048 cm)	1.40 in. (3.556 cm)	1.60 in. (4.064 cm)	1.80 in. (4.572 cm)
AM 350 (CRT); S _m = 40 ksi (276 MN/m ²)																
80	300	60	414	780	2 000	2 650	3 050	3 350	3 525	3 650	3 725					
80	300	40	276	1 500	4 250	6 350	7 800	8 775								
80	300	20	138	3 600	9 400	13 800	17 100	19 800								
80	300	10	69	15 000	37 000	53 000	65 500	75 000	82 000	87 500	93 000	98 000	107 000	113 500	570 000	580 000
80	300	a ₅	35	80 000	195 000	270 000	320 000	365 000	405 000	435 000	455 000	480 000	515 000	545 000		
550	561	60	414	315	710	890										
550	561	40	276	1 500	750	1 825	2 075	2 200								
550	561	20	138	3 900	8 750											
550	561	10	69	20 500	44 000	57 500	67 500	75 000	81 000	85 500	89 000	92 000				
550	561	a ₅	35	85 000	205 000	300 000	370 000	425 000	460 000	495 000	525 000	550 000	590 000	620 000	640 000	655 000
-109	195	60	414	1 150	2 900	4 000										
-109	195	40	276	2 500	5 650	6 500										
-109	195	20	138	6 250	14 750	20 750	24 750	28 000								
-109	195	10	69	28 000	61 000	83 000	99 000	111 000	122 000	132 000	140 000	147 000	158 000	166 000	172 000	
-109	195	a ₅	35	320 000	575 000	710 000	800 000	865 000	920 000	960 000	985 000	1 010 000	1 050 000	1 080 000	1 100 000	1 116 000
AM 367; S _m = 40 ksi (276 MN/m ²)																
80	300	40	276	3 500	7 500	8 400										
80	300	20	138	11 000	25 500	34 500	40 500	45 000								
80	300	10	69	35 000	85 000	120 000	147 000	170 000	190 000	206 000	220 000	232 000	250 000	263 000	272 000	277 000
550	561	40	276	2 100	3 900											
550	561	20	138	13 000	26 000	35 000	40 500	43 000								
-109	195	40	276	5 500	8 500											
-109	195	20	138	10 700	27 700	39 900	42 200	46 500								
-109	195	10	69	71 000	157 000	214 000	258 000	289 000	315 000							
Inconel 718; S _m = 40 ksi (276 MN/m ²)																
80	300	60	414	940	2 060	2 650										
80	300	40	276	2 400	5 600	7 500	8 800	9 600								
80	300	20	138	7 000	18 500	28 000	34 500	39 500	43 000	46 000						
80	300	10	69	59 000	130 000	177 000	211 000	238 000	258 000	274 000	288 000	299 000	317 000	331 000	2 910 000	2 940 000
80	300	a ₅	35	800 000	1 580 000	1 960 000	2 180 000	2 330 000	2 450 000	2 550 000	2 620 000	2 690 000	2 780 000	2 860 000		
550	561	60	414	960	2 000	2 560										
550	561	40	276	1 850	4 650	6 100	7 000									
550	561	20	138	7 500	17 000	23 000	27 100	30 100								
550	561	10	69	25 000	62 000	91 000	113 000	131 000	143 000	153 000	162 000	170 000	181 000			
550	561	a ₅	35	135 000	320 000	440 000	520 000	580 000	630 000	665 000	695 000	720 000	760 000	790 000	815 000	830 000
-109	195	60	414	1 400	2 950	3 600										
-109	195	40	276	3 100	7 100	9 700										
-109	195	20	138	11 000	25 500	35 000	41 500	47 000	51 500	55 000						
-109	195	10	69	58 000	133 000	181 000	217 000	245 000	268 000	286 000	302 000	314 000	334 000	350 000		
-109	195	a ₅	35	3 410 000	3 874 000	4 060 000	4 177 000	4 261 000	4 323 000	4 375 000	4 419 000	4 456 000	4 519 000	4 560 000	4 588 000	4 605 000
Ti-8Al-1Mo-1V; duplex annealed; t = 0.250 in. (6.350 mm); S _m = 25 ksi (173 MN/m ²)																
80	300	25	173	400	780	970										
80	300	15	104	1 900	3 730	4 650	5 210	5 550								
80	300	10	69	5 800	12 200	17 000	20 000									
80	300	5	35	195 000	375 000	411 000	435 000	450 000	460 000	465 000	470 000					
80	300	b ₂	14	1 250 000	2 750 000	3 676 000	4 350 000	4 900 000	5 325 000	5 675 000	5 875 000	5 975 000	6 075 000	6 150 000	6 175 000	6 200 000
550	561	25	173	1 340	3 290	4 450										
550	561	15	104	2 650	7 450	10 850	12 850	14 350								
550	561	10	69	8 500	20 000	28 000	33 900	38 500	42 400	45 300						
550	561	5	35	130 000	312 000	385 000	427 000	452 000	475 000	495 000	510 000	525 000	548 000	560 000		
550	561	b ₂	14	410 000	1 120 000	1 720 000	2 230 000	2 660 000	3 010 000	3 310 000	3 570 000	3 830 000	4 290 000	4 670 000	4 900 000	5 010 000
-109	195	25	173	220	475	662										
-109	195	15	104	2 550	3 680	4 000	4 200	4 290								
-109	195	10	69	8 000	14 500	16 500										
-109	195	5	35	54 000	130 000	172 000	189 000	199 000	204 000	208 000						
-109	195	b ₂	14													
No data available																

^aCrack initiated at S_a of 10 ksi (69 MN/m²) to expedite testing.

^bCrack initiated at S_a of 5 ksi (35 MN/m²) to expedite testing.

TABLE IV.- MEAN NUMBER OF CYCLES REQUIRED TO EXTEND CRACKS FROM A HALF-LENGTH OF 0.15 INCH (0.38 cm) - Concluded

Temperature		S _a		Number of cycles required to propagate a crack from a half length a of 0.15 inch (0.38 cm) to a length a of -												
°F	°K	ksi	MN/m ²	0.20 in. (0.508 cm)	0.30 in. (0.762 cm)	0.40 in. (1.016 cm)	0.50 in. (1.270 cm)	0.60 in. (1.524 cm)	0.70 in. (1.778 cm)	0.80 in. (2.032 cm)	0.90 in. (2.286 cm)	1.00 in. (2.540 cm)	1.20 in. (3.048 cm)	1.40 in. (3.556 cm)	1.60 in. (4.064 cm)	1.80 in. (4.572 cm)
Ti-8Al-1Mo-1V; duplex annealed; t = 0.050 in. (1.270 mm)																
80	300	25	173	1 750	3 700	4 900										
80	300	15	104	4 300	10 500	14 300	17 000									
80	300	10	69	8 000	19 500	28 000	34 000	38 500	42 000	45 000						
80	300	5	35	75 000	155 000	200 000	240 000	265 000	300 000	300 000	310 000	320 000	330 000			
80	300	b ₂	14	660 000	1 800 000	2 645 000	3 280 000	3 700 000	4 020 000	4 280 000	4 460 000	4 590 000	4 770 000	4 900 000	4 980 000	5 050 000
550	561	25	173	2 900	6 500	8 900										
550	561	15	104	6 200	14 900	20 900	25 600	29 400								
550	561	10	69	13 500	31 500	42 500	51 000	58 000	64 000	69 500	74 000					
550	561	5	35	74 000	184 000	252 000	300 000	336 000	367 000	389 000	409 000	427 000	454 000			
550	561	b ₂	14	708 000	1 018 000	1 298 000	1 428 000	1 563 000	1 685 000	1 788 000	1 868 000	1 943 000	2 048 000	2 123 000	2 168 000	2 193 000
-109	195	25	173	1 075	2 275	3 025										
-109	195	15	104	4 900	10 500	13 500										
-109	195	10	69	9 800	21 000	28 000	32 600									
-109	195	5	35	97 000	195 000	249 000	282 000	304 000	319 000	330 000	340 000	348 000	360 000	368 000		
-109	195	b ₂	14	1 502 000	2 752 000	3 372 000	3 742 000	3 962 000	4 112 000	4 222 000	4 312 000	4 382 000	4 472 000	4 522 000	4 552 000	4 572 000
2020-T6; S _m = 15 ksi (104 MN/m ²)																
80	300	15	104	500												
80	300	10	69	1 250												
80	300	5	35	11 500			36 000									
80	300	3.5	24	38 000		33 000	38 000	89 500								
80	300	b ₂	14	228 000	460 000	560 000	610 000	636 000	656 000	665 000	673 000	676 000				
250	394	15	104	700	1 200	1 450										
250	394	10	69	1 300	2 400	2 900	3 200	3 400	3 450							
250	394	5	35	14 500	30 000	37 500	40 500									
250	394	3.5	24	43 000	83 000	104 000	117 000	124 000	129 000							
250	394	b ₂	14	290 000	595 000	770 000	870 000	920 000	965 000	990 000	1 010 000	1 030 000	1 053 000	1 070 000	1 075 000	
-109	195	15	104	340												
-109	195	10	69													
-109	195	5	35	11 900	24 100	27 900										
-109	195	3.5	24	39 000	76 000	90 000	96 000	97 000								
-109	195	b ₂	14	345 000	635 000	750 000	807 000	835 000	853 000							
2024-T81 (clad); S _m = 15 ksi (104 MN/m ²)																
80	300	15	104	640	1 340	1 670										
80	300	10	69	1 600	3 650	4 850	5 600	6 050	6 300							
80	300	5	35	12 000	26 000	34 000	40 000	43 500								
80	300	3.5	24	40 000	83 000	103 000	116 000	126 000	132 000	137 000						
80	300	b ₂	14	290 000	630 000	810 000	880 000	930 000	965 000	990 000	1 010 000	1 030 000	1 053 000	1 070 000	1 077 000	
250	394	15	104	430	890	1 080										
250	394	10	69	1 600	3 400	4 500	5 300	5 700	6 000	6 300						
250	394	5	35	10 000	21 500	27 500	31 500	34 000								
250	394	3.5	24	31 000	71 000	96 000	110 000	119 000	126 000	132 000	138 000	141 000	825 000	845 000	855 000	
250	394	b ₂	14	230 000	475 000	580 000	650 000	700 000	730 000	755 000	770 000	800 000				
-109	195	15	104	855	1 775	2 250										
-109	195	10	69	2 100	4 200	5 400	6 100	6 600	6 900							
-109	195	5	35	12 000	26 500	35 000	40 100	43 000								
-109	195	3.5	24	46 000	88 000	112 500	129 500	140 000	148 000	154 000	158 000	165 000	998 000	1 005 000		
-109	195	b ₂	14	265 000	600 000	740 000	815 000	865 000	902 000	928 000	953 000	965 000	986 000	998 000	1 005 000	
RR-58 (clad); S _m = 15 ksi (104 MN/m ²)																
80	300	15	104	660	1 400	1 750	1 960	2 080	2 120							
80	300	10	69	1 510	3 270	4 130	4 620	4 920	5 120	5 300	5 380					
80	300	5	35	14 000	28 000	37 000	42 000	45 000								
80	300	3.5	24	29 000	63 000	81 000	94 000	103 000	109 000	112 000						
80	300	b ₂	14	138 000	290 000	380 000	440 000	480 000	510 000	533 000	551 000	565 000	586 000	600 000	608 000	
250	394	15	104	470	1 000	1 240	1 370	1 450	1 510							
250	394	10	69	1 080	2 120	2 710	3 080	3 300	3 430	3 520	3 580					
250	394	5	35	14 000	28 500	37 000	41 000	43 000								
250	394	3.5	24	45 000	98 000	124 000	139 000	148 000	151 000	154 000						
250	394	b ₂	14	430 000	1 110 000	1 490 000	1 730 000	1 920 000	2 040 000	2 115 000	2 185 000	2 230 000	2 290 000	2 330 000	2 350 000	2 360 000
-109	195	15	104	740	1 500	1 780	1 910	1 980								
-109	195	10	69	1 120	2 300	3 000	3 390	3 610	3 750	3 820						
-109	195	5	35	13 500	29 500	38 000	43 200	46 700								
-109	195	3.5	24	48 000	90 000	112 000	127 000	137 000	144 600	148 500	151 000	153 000	1 248 000	1 260 000		
-109	195	b ₂	14	500 000	890 000	1 020 000	1 090 000	1 136 000	1 170 000	1 190 000	1 210 000	1 230 000				

^bCrack initiated by S_a of 5 ksi (35 MN/m²) to expedite testing.
^cCrack initiated at S_a of 3.5 ksi (24 MN/m²) to expedite testing.

2/22/85
ep

"The aeronautical and space activities of the United States shall be conducted so as to contribute . . . to the expansion of human knowledge of phenomena in the atmosphere and space. The Administration shall provide for the widest practicable and appropriate dissemination of information concerning its activities and the results thereof."

—NATIONAL AERONAUTICS AND SPACE ACT OF 1958

NASA SCIENTIFIC AND TECHNICAL PUBLICATIONS

TECHNICAL REPORTS: Scientific and technical information considered important, complete, and a lasting contribution to existing knowledge.

TECHNICAL NOTES: Information less broad in scope but nevertheless of importance as a contribution to existing knowledge.

TECHNICAL MEMORANDUMS: Information receiving limited distribution because of preliminary data, security classification, or other reasons.

CONTRACTOR REPORTS: Technical information generated in connection with a NASA contract or grant and released under NASA auspices.

TECHNICAL TRANSLATIONS: Information published in a foreign language considered to merit NASA distribution in English.

TECHNICAL REPRINTS: Information derived from NASA activities and initially published in the form of journal articles.

SPECIAL PUBLICATIONS: Information derived from or of value to NASA activities but not necessarily reporting the results of individual NASA-programmed scientific efforts. Publications include conference proceedings, monographs, data compilations, handbooks, sourcebooks, and special bibliographies.

Details on the availability of these publications may be obtained from:

SCIENTIFIC AND TECHNICAL INFORMATION DIVISION
NATIONAL AERONAUTICS AND SPACE ADMINISTRATION
Washington, D.C. 20546